Acta Cryst E CRYSTALLOGRAPHIC COMMUNICATIONS

ISSN 2056-9890

Hirshfeld analysis and molecular docking with the RDR enzyme of 2-(5-chloro-2-oxoindolin-3-ylidene)-*N*-methylhydrazinecarbothioamide

Jecika Maciel Velasques,[a]‡ Vanessa Carratu Gervini,[a]* Lisliane Kickofel,[a] Renan Lira de Farias[b] and Adriano Bof de Oliveira[c]

[a]Universidade Federal do Rio Grande (FURG), Escola de Química e Alimentos, Rio Grande, Brazil, [b]Universidade Estadual Paulista (UNESP), Instituto de Química, Araraquara, Brazil, and [c]Universidade Federal de Sergipe (UFS), Departamento de Química, São Cristóvão, Brazil. *Correspondence e-mail: vanessa.gervini@gmail.com

Received 4 April 2017
Accepted 10 April 2017

Edited by H. Stoeckli-Evans, University of Neuchâtel, Switzerland

‡ Current address: Universidade Estadual Paulista (UNESP), Instituto de Química, Araraquara, Brazil.

Keywords: crystal structure; isatin thiosemicarbazone derivative; hydrogen bonding; Hirshfeld surface analysis; RDR-thiosemicarbazone *in silico* evaluation.

CCDC reference: 1543340

Supporting information: this article has supporting information at journals.iucr.org/e

The acetic acid-catalyzed reaction between 5-chloroisatin and 4-methylthiosemicarbazide yields the title compound, $C_{10}H_9ClN_4OS$ (I) (common name: 5-chloroisatin-4-methylthiosemicarbazone). The molecule is nearly planar (r.m.s. deviation = 0.047 Å for all non-H atoms), with a maximum deviation of 0.089 (1) Å for the O atom. An *S*(6) ring motif formed by an intramolecular N—H···O hydrogen bond is observed. In the crystal, molecules are linked by N—H···O hydrogen bonds, forming chains propagating along the *a*-axis direction. The chains are linked by N—H···S hydrogen bonds, forming a three-dimensional supramolecular structure. The three-dimensional framework is reinforced by C—H···π interactions. The absolute structure of the molecule in the crystal was determined by resonant scattering [Flack parameter = 0.006 (9)]. The crystal structure of the same compound, measured at 100 K, has been reported on previously [Qasem Ali *et al.* (2012). *Acta Cryst.* E**68**, o964–o965]. The Hirshfeld surface analysis indicates that the most important contributions for the crystal packing are the H···H (23.1%), H···C (18.4%), H···Cl (13.7%), H···S (12.0%) and H···O (11.3%) interactions. A molecular docking evaluation of the title compound with the ribonucleoside diphosphate reductase (RDR) enzyme was carried out. The title compound (I) and the active site of the selected enzyme show Cl···H—C*(LYS140)*, *Cg*(aromatic ring)···H—C*(SER71)*, H···O—C*(GLU200)* and Fe^{III}···O···Fe^{III} intermolecular interactions, which suggests a solid theoretical structure–activity relationship.

1. Chemical context

Methods for the synthesis of isatin derivatives were first reported in the first half of the 19th century (Erdmann, 1841*a*,*b*; Laurent, 1841), while for thiosemicarbazone derivatives one of the first reports can be traced back to the early 1900's (Freund & Schander, 1902). Initially, thiosemicarbazone chemistry was not related to the pharmacological sciences. This has changed since the discovery that *in vitro* assays of sulfur-containing compounds showed that they are effective for *Mycobacterium tuberculosis* growth inhibition (Domagk *et al.*, 1946). In the 1950's, the synthesis of isatin–thiosemicarbazone derivatives was reported (Campaigne & Archer, 1952) and *in vitro* assays indicated such compounds to be active against Cruzain, Falcipain-2 and Rhodesian (Chiyanzu *et al.*, 2003). Nowadays, many isatin–thiosemicarbazone derivatives employed in medicinal chemistry. For example, 1-[(2-methylbenzimidazol-1-yl) methyl]-2-oxo-indolin-3-ylidene]amino]thiourea is an *in vitro* and *in silico*

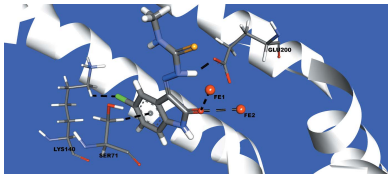

Chikungunya virus inhibitor (Mishra *et al.*, 2016). The title compound (I), 5-chloroisatin-4-methylthiosemicarbazone, is an intermediate in the synthetic pathway of HIV-1 (human immunodeficiency virus type 1) RT (reverse transcriptase) inhibitor synthesis (Meleddu *et al.*, 2017); a new crystal structure determination is reported here, the original work having been published by Qasem Ali *et al.* (2012). Thus, the crystal structure determination of isatin–thiosemicarbazone-based molecules is an intensive research area in medicinal chemistry and the main focus of our work.

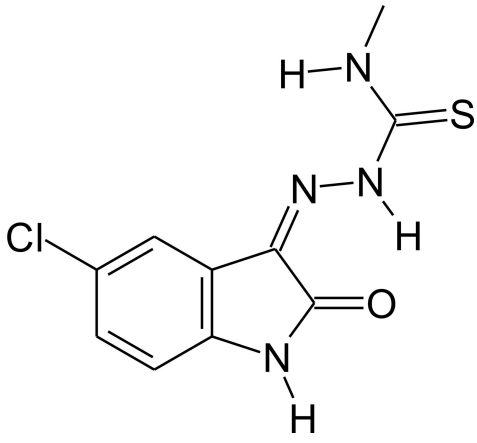

2. Structural commentary

The present analysis of the title compound (I), measured at 200 K, is very similar to that measured by Qasem Ali *et al.* (2012) at 100 K. There is one intramolecular hydrogen bond, N3—H3*N*···O1 (Table 1), with an *S*(6) graph-set motif (Fig. 1).

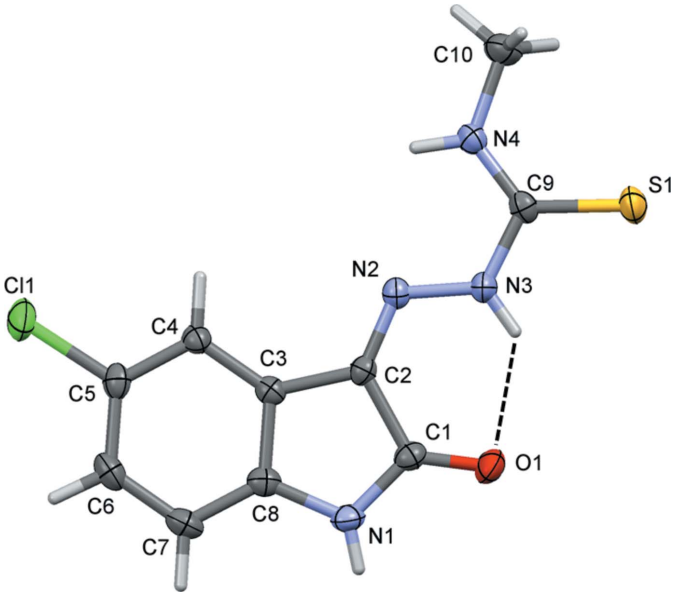

Figure 1
The molecular structure of the title compound (I) (this work), showing the atom labelling and displacement ellipsoids drawn at the 50% probability level. The intramolecular hydrogen bond [graph-set motif *S*(6)] is shown as a dashed line (see Table 1).

Table 1
Hydrogen-bond geometry (Å, °).

Cg is the centroid of the C3–C8 ring.

D—H···*A*	*D*—H	H···*A*	*D*···*A*	*D*—H···*A*
N3—H3*N*···O1	0.83 (2)	2.12 (3)	2.756 (2)	134 (2)
N1—H1*N*···O1^{i}	0.79 (2)	2.04 (3)	2.824 (2)	175 (2)
N4—H4*N*···S1^{ii}	0.88 (3)	2.72 (3)	3.518 (2)	152 (2)
C6—H6···*Cg*^{iii}	0.95	2.61	3.410 (2)	142

Symmetry codes: (i) $x+\frac{1}{2}, -y+\frac{3}{2}, -z+1$; (ii) $-x, y-\frac{1}{2}, -z+\frac{3}{2}$; (iii) $x+\frac{1}{2}, -y+\frac{1}{2}, -z+1$.

The molecule is almost planar (r.m.s. deviation = 0.047 Å for all non-H atoms), with maximum deviations of −0.089 (1), −0.073 (1) and 0.057 (1) Å for atoms O1, Cl1 and S1, respectively. In addition, the torsion angle for the N4—C9—N3—N2 unit is −0.8 (2)°.

3. Supramolecular features

In the crystal, molecules are linked by N1—H1*N*···O1^{i} hydrogen bonds, forming chains propagating along the *a*-axis direction. The chains are linked by N4—H4*N*···S^{ii} hydrogen bonds, forming a three-dimensional supramolecular structure (Fig. 2, Table 1). The three-dimensional framework is reinforced by C6—H6···π^{iii} interactions, as shown in Fig. 2 (see also Table 1). The crystal structure determined in this work and that of the originally published article (Qasem Ali *et al.*, 2012) are, of course, similar.

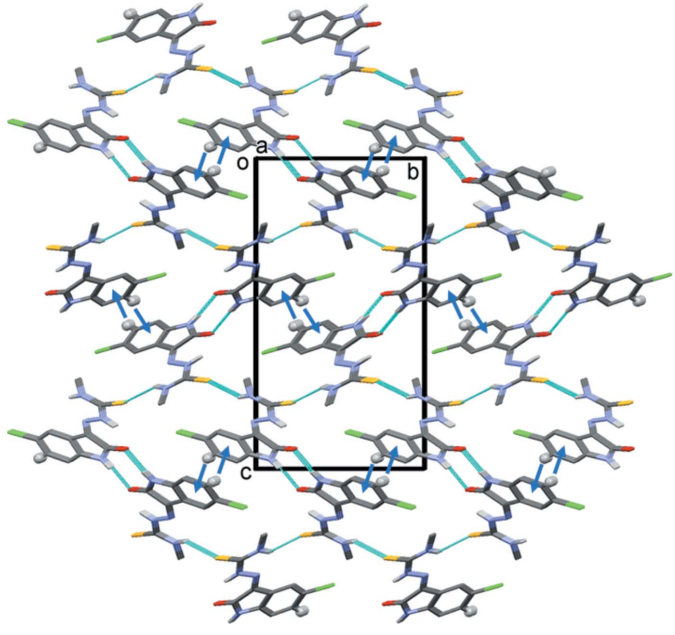

Figure 2
A view along the *a* axis of the crystal packing of the title compound (I) (this work). Details of the N—H···O and N—H···S hydrogen bonds (dashed lines) and the C—H···π interactions (blue arrows) are given in Table 1. H atoms not involved in these interactions have been omitted for clarity.

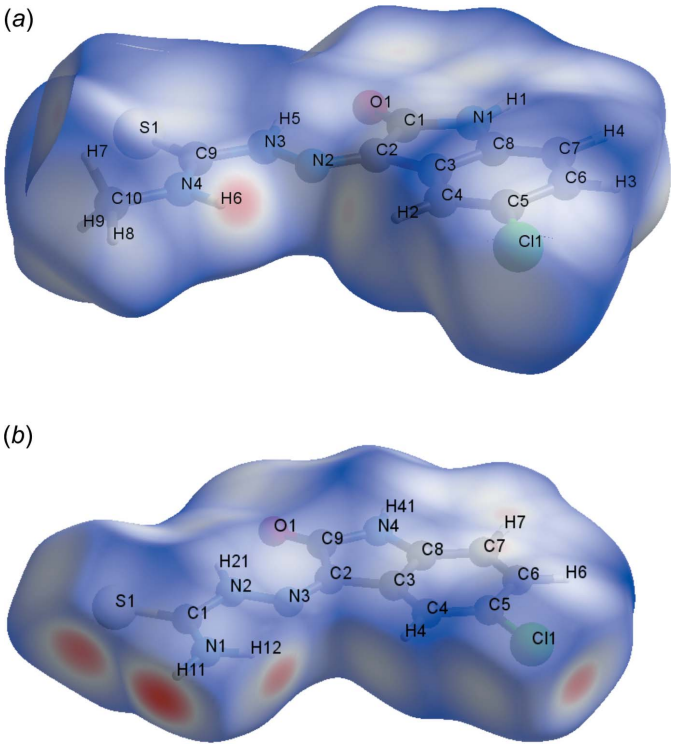

Figure 3
The Hirshfeld surface graphical representation (d_{norm}) for the asymmetric unit of: (*a*) the title compound (I) (this work) and (*b*) 5-chloroisatin-thiosemicarbazone (II) (de Bittencourt *et al.*, 2014). The surface regions with strongest intermolecular interactions are drawn in magenta colour.

4. Hirshfeld surface analysis

The Hirshfeld surface analysis (Hirshfeld, 1977) of the crystal structure of (I) suggests that the contribution of the H···H intermolecular interactions for the crystal structure cohesion amounts to 23.1%. The contributions of the other major intermolecular interactions are: H···C (18.4%), H···Cl (13.7%), H···S (12.0%) and H···O (11.3%). The minor observed contributions for the crystal packing are H···N (5.3%) and C···N (4.2%). The Hirshfeld surface graphical representation, d_{norm}, with transparency and labelled atoms indicates, in magenta, the locations of the strongest intermolecular contacts, *e.g.* the H6 and H2 atoms, which are important for the intermolecular hydrogen bonding (Fig. 3*a*). The H···H, H···C, H···Cl, H···S and H···O contributions to the crystal packing are shown as a Hirshfeld surface two-dimensional fingerprint plot with cyan dots. The d_e (*y* axis) and d_i (*x* axis) values are the closest external and internal distances (Å) from given points on the Hirshfeld surface contacts (Figs. 4*a* and 5) (Wolff *et al.*, 2012).

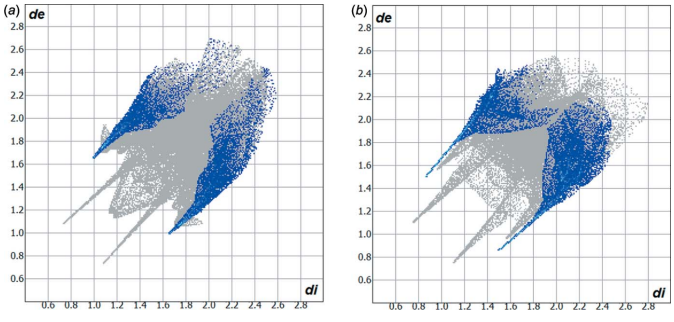

Figure 4
Hirshfeld surface two-dimensional fingerprint plots for the crystal structures of: (*a*) the title compound (I) (this work) and (*b*) 5-chloroisatin-thiosemicarbazone (II) (de Bittencourt *et al.*, 2014), showing the H···S contacts in detail (cyan dots). The contribution of the H···S interactions to the molecular cohesion of the crystal structures amounts to 12.0 and 17.2%, respectively. The d_e (*y* axis) and d_i (*x* axis) values are the closest external and internal distances (Å) from given points on the Hirshfeld surface contacts.

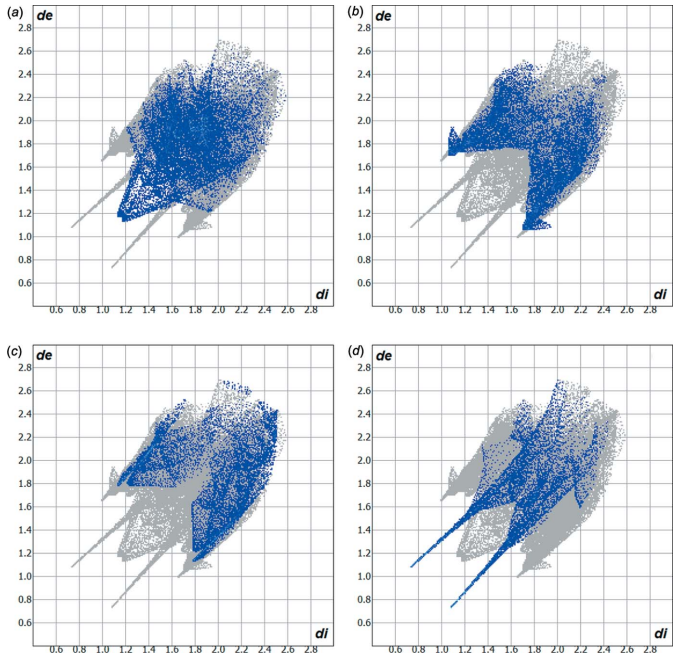

Figure 5
Hirshfeld surface two-dimensional fingerprint plots for the title compound (I) (this work), showing the (*a*) H···H, (*b*) H···C, (*c*) H···Cl and (*d*) H···O contacts in detail (cyan dots). The contributions of the interactions to the crystal packing amount to 23.1, 18.4, 13.7 and 11.3%, respectively. The d_e (*y* axis) and d_i (*x* axis) values are the closest external and internal distances (Å) from given points on the Hirshfeld surface contacts.

5. Molecular docking

Finally, for an interaction between the 5-chloroisatin-4-methylthiosemicarbazone (this work) and a biological target, the ribonucleoside diphosphate reductase (RDR), a lock-and-key supramolecular analysis was carried out (Chen, 2015). The RDR enzyme was selected for this work due its importance in cell proliferation. It catalyzes the conversion of ribonucleotides to deoxyribonucleotides, which is the rate-limiting step for DNA synthesis. In addition, a thiosemicarbazone derivative, the 3-amino-pyridine-2-carboxaldehyde thiosemicarbazone, shows RDR inhibition and biological activity is suggested by its coordination with the Fe ions of the enzyme

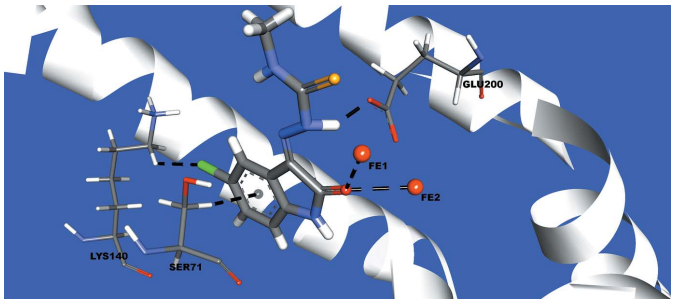

Figure 6
Graphical representation of a lock-and-key model for the title compound (I) (this work) and the RDR enzyme active site, with selected amino acid residues. The interactions are shown as dashed lines and the figure in the stick model is simplified for clarity.

active site (Popović-Bijelić *et al.*, 2011). The commercial name for this thiosemicarbazone derivative is Triapine. Its source until 2009 was Vion Pharmaceuticals Inc., New Haven, CT, United States. Since 2017, Trethera Corporation, Santa Monica, CA, and Nanotherapeutics Inc., Alachua, FL, have had a worldwide agreement for the development, production and commercialization of Triapine formulations and for its applications in hematological malignancies (Nanotherapeutics, 2017). This illustrates that academic institutions, public and private research facilities and industry have a high level of interest in thiosemicarbazone derivatives and in studies concerning RDR–thiosemicarbazone interactions.

The semi-empirical equilibrium energy of the title compound (this work) was obtained using the PM6 Hamiltonian (Stewart, 2013), but the experimental bond lengths were conserved. The crystal structure of the RDR enzyme (PDB code: 1W68) was downloaded from the Protein Data Bank (Strand *et al.*, 2004). The calculated parameters were: heat of formation = 98.697 kcal mol^{-1}, gradient normal = 0.68005, HOMO = −8.934 eV, LUMO = −1.598 eV and energy gap = 7.336 eV. The title compound (I) and the active site of the selected enzyme matches and structure–activity relationship can be assumed by the following observed intermolecular interactions: Cl1···H—C*(LYS140)* = 2.538 Å, *Cg*(aromatic ring)···H—C*(SER71)* = 2.714 Å, H5···O—C*(GLU200)* = 1.663 Å, Fe1···O1 = 2.567 Å and Fe2···O1 = 2.511 Å. The *in silico* evaluation suggests through the graphical representation the bridging O1 atom connecting the two Fe^{III} metal centers by intermolecular interactions (Fig. 6).

6. Comparison with a related structure

Isatin–thiosemicarbazone derivatives have molecular structural features in common, *viz.* nearly a planar geometry as a result of the sp^2-hybridized C and N atoms of the main fragment. For a comparison with the title compound [5-chloroisatin-4-methylthiosemicarbazone (I); this work], 5-chloroisatin-thiosemicarbazone, (II), was selected (de Bittencourt *et al.*, 2014) as both structures have the same main entity. The molecular structural difference is the substitution of one H atom of the amine group of (II) by a methyl group in the title compound (I). Although the molecular basis for the two compounds is the same, there are significant differences in the crystal packing. For compound (I), the unit cell is chiral and the molecules are linked by hydrogen bonding into a three-dimensional network (Figs. 2 and 7*a*), while for compound (II) the unit cell is centrosymmetric and the hydrogen bonding is observed in a planar arrangement, with the molecules stacked along the [001] direction (Fig. 7*b*). The terminal methyl group in (I) decreases the possibility of H-atom contacts with S and O acceptors, while in compound (II), the presence of the terminal unsubstituted amine increases the chances for hydrogen bonding, as suggested by the Hirshfeld surface analysis, d_{norm}, for the two molecules (Fig. 3*a*,*b*). The Hirshfeld surface two-dimensional fingerprint plot shows that the contribution of the H···S intermolecular interaction to the crystal cohesion amounts to 12.0% in the title compound (I), while for the 5-chloroisatin-thiosemicarbazone (II) it amounts to 17.2% (Fig. 5*a*,*b*). The relationship between thio-

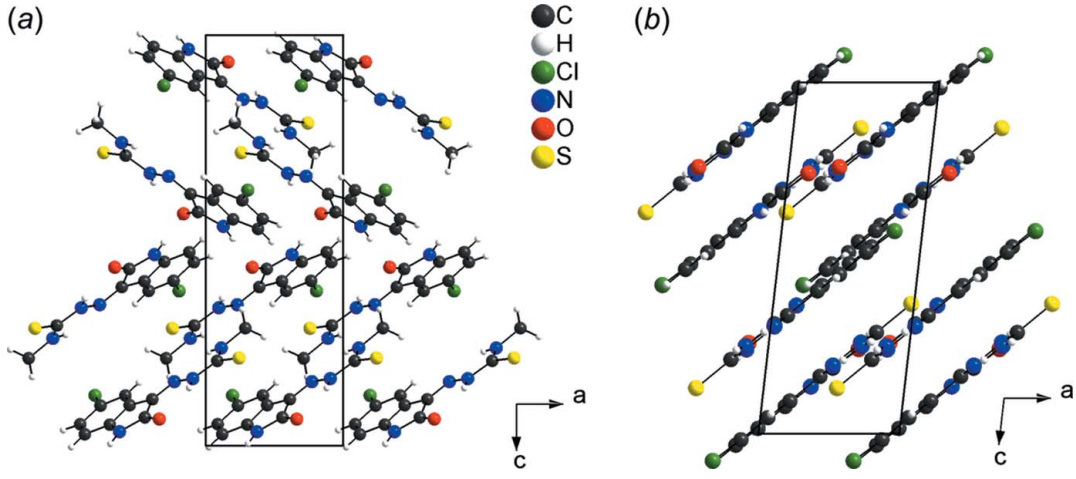

Figure 7
Section of the crystal structures of: (*a*) the title compound (I) (this work), and (*b*) 5-chloroisatin–thiosemicarbazone (II) (de Bittencourt *et al.*, 2014), showing the molecular stacking along the [001] direction. The crystal packing of both compounds is viewed along the *b* axis, and the figures are simplified for clarity.

Table 2
Experimental details.

Crystal data	
Chemical formula	$C_{10}H_9ClN_4OS$
M_r	268.72
Crystal system, space group	Orthorhombic, $P2_12_12_1$
Temperature (K)	200
a, b, c (Å)	6.2584 (1), 10.1734 (2), 18.7183 (3)
V (Å^3)	1191.78 (4)
Z	4
Radiation type	Mo $K\alpha$
μ (mm^{-1})	0.48
Crystal size (mm)	0.46 × 0.16 × 0.12
Data collection	
Diffractometer	Bruker APEXII CCD area detector
Absorption correction	Multi-scan (*SADABS*; Bruker, 2014)
T_{min}, T_{max}	0.697, 0.749
No. of measured, independent and observed [$I > 2\sigma(I)$] reflections	10426, 2342, 2295
R_{int}	0.013
(sin $\theta/\lambda)_{max}$ (Å^{-1})	0.617
Refinement	
$R[F^2 > 2\sigma(F^2)]$, $wR(F^2)$, S	0.020, 0.056, 1.05
No. of reflections	2342
No. of parameters	167
H-atom treatment	H atoms treated by a mixture of independent and constrained refinement
$\Delta\rho_{max}$, $\Delta\rho_{min}$ (e Å^{-3})	0.19, −0.15
Absolute structure	Flack x determined using 940 quotients $[(I^+)-(I^-)]/[(I^+)+(I^-)]$ (Parsons *et al.*, 2013)
Absolute structure parameter	0.006 (9)

Computer programs: *APEX2* and *SAINT* (Bruker, 2014), *SHELXT2014* (Sheldrick, 2015*a*), *SHELXL2016* (Sheldrick, 2015*b*), *Mercury* (Macrae *et al.*, 2008), *DIAMOND* (Brandenburg, 2006), *GOLD* (Chen, 2015), *MOPAC* (Stewart, 2013), *Crystal Explorer* (Wolff *et al.*, 2012), *publCIF* (Westrip, 2010) and *enCIFer* (Allen *et al.*, 2004).

semicarbazone derivatives, the molecular assembly, the geometry of the H···S interactions and their contribution to the crystal structures can be seen in a recently published article (de Oliveira *et al.*, 2017).

7. Synthesis and crystallization

The starting materials are commercially available and were used without further purification. The synthesis of the title compound was adapted from a previously reported procedure (Freund & Schander, 1902). In an acetic acid-catalyzed reaction, a mixture of 5-cloroisatin (3 mmol) and 4-methyl-3-thiosemicarbazide (3 mmol) in ethanol (40 ml) was stirred and refluxed for 5 h. On cooling, a solid was obtained which was filtered off. Yellow prismatic crystals of the title compound were grown in tetrahydrofuran by slow evaporation of the solvent.

8. Refinement

Crystal data, data collection and structure refinement details for the title compound (I) are summarized in Table 2. The NH H atoms were located in difference-Fourier maps and freely refined. The C-bound H atoms were positioned with idealized geometry and refined using a riding model: C—H = 0.95–0.98 Å with U_{iso}(H) = 1.5U_{eq}(C-methyl) and 1.2U_{eq}(C) for other H atoms. The absolute structure of the molecule in the crystal was determined by resonant scattering [Flack parameter = 0.006 (9)].

Acknowledgements

ABO is an associate researcher in the project 'Dinitrosyl complexes containing thiol and/or thiosemicarbazone: synthesis, characterization and treatment against cancer', founded by FAPESP, Proc. 2015/12098–0, and acknowledges Professor José C. M. Pereira (São Paulo State University, Brazil) for his support in this work. ABO also acknowledges VCG for the invitation to be a visiting professor at the Federal University of Rio Grande, Brazil, where part of this work was developed. JMV and RLF thank the CAPES foundation for the scholarships. The authors acknowledge Professor A. J. Bortoluzzi for access to the experimental facilities and the data collection (Federal University of Santa Catarina, Brazil).

References

Allen, F. H., Johnson, O., Shields, G. P., Smith, B. R. & Towler, M. (2004). *J. Appl. Cryst.* **37**, 335–338.
Bittencourt, V. C. D. de, Vicenti, J. R. de M., Velasques, J. M., Zambiazi, P. J. & Gervini, V. C. (2014). *Acta Cryst.* E**70**, o64–o65.
Brandenburg, K. (2006). *DIAMOND*. Crystal Impact GbR, Bonn, Germany.
Bruker (2014). *APEX2*, *SAINT* and *SADABS*. Bruker AXS Inc., Madison, Wisconsin, USA.
Campaigne, E. & Archer, W. L. (1952). *J. Am. Chem. Soc.* **74**, 5801.
Chen, Y.-C. (2015). *Trends Pharmacol. Sci.* **36**, 78–95.
Chiyanzu, I., Hansell, E., Gut, J., Rosenthal, P. J., McKerrow, J. H. & Chibale, K. (2003). *Bioorg. Med. Chem. Lett.* **13**, 3527–3530.
Domagk, G., Behnisch, R., Mietzsch, F. & Schmidt, H. (1946). *Naturwissenschaften*, **33**, 315.
Erdmann, O. L. (1841*a*). *Ann. Chim. Phys.* **3**, 355–371.
Erdmann, O. L. (1841*b*). *J. Prakt. Chem.* **22**, 257–299.
Freund, M. & Schander, A. (1902). *Ber. Dtsch. Chem. Ges.* **35**, 2602–2606.
Hirshfeld, H. L. (1977). *Theor. Chim. Acta*, **44**, 129–138.
Laurent, A. (1841). *Ann. Chim. Phys.* **3**, 371–383.
Macrae, C. F., Bruno, I. J., Chisholm, J. A., Edgington, P. R., McCabe, P., Pidcock, E., Rodriguez-Monge, L., Taylor, R., van de Streek, J. & Wood, P. A. (2008). *J. Appl. Cryst.* **41**, 466–470.
Meleddu, R., Distinto, S., Corona, A., Tramontano, E., Bianco, G., Melis, C., Cottiglia, F. & Maccioni, E. (2017). *J. Enzyme Inhib. Med. Chem.* **32**, 130–136.
Mishra, P., Kumar, A., Mamidi, P., Kumar, S., Basantray, I., Saswat, T., Das, I., Nayak, T. K., Chattopadhyay, S., Subudhi, B. B. & Chattopadhyay, S. (2016). *Sci. Rep.* **6**, 20122.
Nanotherapeutics (2017). http://www.nanotherapeutics.com/news/ or http://www.businesswire.com/news/home/20170105005197/en/Trethera-Corporation-Nanotherapeutics-Sign-Exclusive-Worldwide-Agreement. Access on April 03, 2017, news from January 05, 2017.
Oliveira, A. B. de, Beck, J., Landvogt, C., de Farias, R. L. & Feitoza, B. R. S. (2017). *Acta Cryst.* E**73**, 291–295.
Parsons, S., Flack, H. D. & Wagner, T. (2013). *Acta Cryst.* B**69**, 249–259.

Popović-Bijelić, A., Kowol, C. R., Lind, M. E. S., Luo, J., Himo, F., Enyedy, É. A., Arion, V. B. & Gräslund, A. (2011). *J. Inorg. Biochem.* **105**, 1422–1431.
Qasem Ali, A., Eltayeb, N. E., Teoh, S. G., Salhin, A. & Fun, H.-K. (2012). *Acta Cryst.* E**68**, o964–o965.
Sheldrick, G. M. (2015*a*). *Acta Cryst.* A**71**, 3–8.
Sheldrick, G. M. (2015*b*). *Acta Cryst.* C**71**, 3–8.
Stewart, J. J. (2013). *J. Mol. Model.* **19**, 1–32.
Strand, K. R., Karlsen, S., Kolberg, M., Røhr, A. K., Görbitz, C. H. & Andersson, K. K. (2004). *J. Biol. Chem.* **279**, 46794–46801.
Westrip, S. P. (2010). *J. Appl. Cryst.* **43**, 920–925.
Wolff, S. K., Grimwood, D. J., McKinnon, J. J., Turner, M. J., Jayatilaka, D. & Spackman, M. A. (2012). *Crystal Explorer*. University of Western Australia, Perth, Australia.

supporting information

Acta Cryst. (2017). E**73**, 702-707 [https://doi.org/10.1107/S2056989017005461]

Hirshfeld analysis and molecular docking with the RDR enzyme of 2-(5-chloro-2-oxoindolin-3-ylidene)-*N*-methylhydrazinecarbothioamide

Jecika Maciel Velasques, Vanessa Carratu Gervini, Lisliane Kickofel, Renan Lira de Farias and Adriano Bof de Oliveira

Computing details

Data collection: *APEX2* (Bruker, 2014); cell refinement: *SAINT* (Bruker, 2014); data reduction: *SAINT* (Bruker, 2014); program(s) used to solve structure: SHELXT2014 (Sheldrick, 2015a); program(s) used to refine structure: *SHELXL2016* (Sheldrick, 2015b); molecular graphics: *Mercury* (Macrae *et al.*, 2008), *DIAMOND* (Brandenburg, 2006), *GOLD* (Chen, 2015), *MOPAC* (Stewart, 2013) and *Crystal Explorer* (Wolff *et al.*, 2012); software used to prepare material for publication: *SHELXL2016* (Sheldrick, 2015b), *publCIF* (Westrip, 2010) and *enCIFer* (Allen *et al.*, 2004).

2-(5-Chloro-2-oxoindolin-3-ylidene)-*N*-methylhydrazinecarbothioamide

Crystal data

$C_{10}H_9ClN_4OS$
M_r = 268.72
Orthorhombic, $P2_12_12_1$
a = 6.2584 (1) Å
b = 10.1734 (2) Å
c = 18.7183 (3) Å
V = 1191.78 (4) Å^3
Z = 4
$F(000)$ = 552
D_x = 1.498 Mg m^{-3}
Mo $K\alpha$ radiation, λ = 0.71073 Å
Cell parameters from 9936 reflections
θ = 3.0–40.9°
μ = 0.48 mm^{-1}
T = 200 K
Prism, yellow
0.46 × 0.16 × 0.12 mm

Data collection

Bruker APEXII CCD area detector diffractometer
Radiation source: fine-focus sealed X-ray tube, Bruker APEXII CCD
φ and ω scans
Absorption correction: multi-scan (SADABS; Bruker, 2014)
T_{min} = 0.697, T_{max} = 0.749
10426 measured reflections
2342 independent reflections
2295 reflections with $I > 2\sigma(I)$
R_{int} = 0.013
θ_{max} = 26.0°, θ_{min} = 2.2°
h = −7→5
k = −12→12
l = −23→23

Refinement

Refinement on F^2
Least-squares matrix: full
$R[F^2 > 2\sigma(F^2)]$ = 0.020
$wR(F^2)$ = 0.056
S = 1.05
2342 reflections
167 parameters
0 restraints
Primary atom site location: structure-invariant direct methods
Secondary atom site location: difference Fourier map
Hydrogen site location: mixed
H atoms treated by a mixture of independent and constrained refinement

$w = 1/[\sigma^2(F_o^2) + (0.0338P)^2 + 0.2804P]$
where $P = (F_o^2 + 2F_c^2)/3$
$(\Delta/\sigma)_{max} = 0.001$
$\Delta\rho_{max} = 0.19$ e Å^{-3}
$\Delta\rho_{min} = -0.15$ e Å^{-3}

Absolute structure: Flack *x* determined using 940 quotients $[(I^+)-(I^-)]/[(I^+)+(I^-)]$ (Parsons *et al.*, 2013)
Absolute structure parameter: 0.006 (9)

Special details

Geometry. All esds (except the esd in the dihedral angle between two l.s. planes) are estimated using the full covariance matrix. The cell esds are taken into account individually in the estimation of esds in distances, angles and torsion angles; correlations between esds in cell parameters are only used when they are defined by crystal symmetry. An approximate (isotropic) treatment of cell esds is used for estimating esds involving l.s. planes.

Fractional atomic coordinates and isotropic or equivalent isotropic displacement parameters (Å²)

	x	*y*	*z*	U_{iso}*/U_{eq}
C1	0.4431 (3)	0.63210 (18)	0.56919 (9)	0.0229 (4)
C2	0.3885 (3)	0.51360 (17)	0.61332 (9)	0.0200 (4)
C3	0.5539 (3)	0.41669 (18)	0.59914 (9)	0.0199 (4)
C4	0.5853 (3)	0.28884 (18)	0.62247 (9)	0.0215 (3)
H4	0.487362	0.247309	0.653982	0.026*
C5	0.7655 (3)	0.22425 (18)	0.59789 (9)	0.0246 (4)
C6	0.9124 (3)	0.2840 (2)	0.55278 (10)	0.0278 (4)
H6	1.036794	0.237337	0.538476	0.033*
C7	0.8793 (3)	0.4117 (2)	0.52828 (10)	0.0271 (4)
H7	0.977419	0.452902	0.496717	0.033*
C8	0.6980 (3)	0.47585 (18)	0.55173 (9)	0.0226 (4)
C9	−0.0829 (3)	0.58961 (18)	0.70690 (9)	0.0216 (4)
C10	−0.2880 (3)	0.4484 (2)	0.78682 (11)	0.0345 (4)
H10A	−0.260071	0.490692	0.832924	0.052*
H10B	−0.301350	0.353251	0.793692	0.052*
H10C	−0.421127	0.483020	0.766648	0.052*
Cl1	0.80561 (8)	0.06052 (5)	0.62274 (3)	0.03753 (15)
N1	0.6267 (3)	0.60279 (16)	0.53459 (8)	0.0254 (3)
H1N	0.684 (4)	0.652 (2)	0.5082 (14)	0.037 (7)*
N2	0.2289 (3)	0.49844 (14)	0.65623 (7)	0.0210 (3)
N3	0.0946 (3)	0.60072 (16)	0.66389 (8)	0.0236 (3)
H3N	0.110 (4)	0.669 (2)	0.6405 (12)	0.031 (6)*
N4	−0.1123 (3)	0.47545 (16)	0.73815 (8)	0.0244 (3)
H4N	−0.014 (4)	0.415 (3)	0.7332 (13)	0.040 (7)*
O1	0.3382 (2)	0.73458 (13)	0.56517 (7)	0.0295 (3)
S1	−0.24203 (8)	0.72186 (5)	0.71392 (3)	0.03074 (13)

Atomic displacement parameters (Å²)

	U^{11}	U^{22}	U^{33}	U^{12}	U^{13}	U^{23}
C1	0.0266 (9)	0.0228 (9)	0.0194 (8)	−0.0015 (7)	−0.0011 (7)	0.0016 (7)
C2	0.0213 (8)	0.0188 (8)	0.0198 (8)	0.0008 (7)	−0.0020 (6)	0.0005 (6)
C3	0.0189 (8)	0.0235 (9)	0.0174 (7)	−0.0005 (7)	−0.0008 (6)	−0.0016 (7)
C4	0.0212 (8)	0.0240 (9)	0.0194 (7)	0.0020 (7)	0.0004 (7)	0.0010 (7)

C5	0.0249 (9)	0.0249 (8)	0.0241 (8)	0.0059 (9)	−0.0053 (7)	−0.0014 (7)
C6	0.0201 (9)	0.0358 (10)	0.0275 (9)	0.0053 (8)	0.0005 (7)	−0.0074 (8)
C7	0.0221 (9)	0.0352 (10)	0.0240 (8)	−0.0047 (8)	0.0051 (7)	−0.0038 (8)
C8	0.0245 (10)	0.0248 (9)	0.0185 (7)	−0.0041 (7)	−0.0002 (7)	−0.0022 (6)
C9	0.0178 (8)	0.0240 (9)	0.0231 (8)	0.0004 (7)	−0.0022 (7)	−0.0042 (7)
C10	0.0261 (10)	0.0391 (11)	0.0382 (10)	−0.0029 (9)	0.0065 (9)	0.0058 (9)
Cl1	0.0386 (3)	0.0307 (3)	0.0433 (3)	0.0154 (2)	−0.0012 (2)	0.0053 (2)
N1	0.0305 (9)	0.0239 (8)	0.0219 (7)	−0.0032 (7)	0.0054 (6)	0.0032 (6)
N2	0.0202 (8)	0.0197 (6)	0.0230 (7)	0.0018 (6)	−0.0012 (6)	−0.0014 (5)
N3	0.0239 (8)	0.0193 (7)	0.0277 (8)	0.0042 (6)	0.0044 (6)	0.0017 (6)
N4	0.0192 (8)	0.0246 (8)	0.0294 (8)	0.0016 (7)	0.0017 (6)	0.0008 (6)
O1	0.0366 (8)	0.0230 (7)	0.0289 (6)	0.0061 (6)	−0.0009 (6)	0.0066 (5)
S1	0.0266 (2)	0.0249 (2)	0.0407 (3)	0.0070 (2)	0.0042 (2)	−0.00341 (19)

Geometric parameters (Å, º)

C1—O1	1.234 (2)	C7—H7	0.9500
C1—N1	1.352 (3)	C8—N1	1.404 (2)
C1—C2	1.501 (2)	C9—N4	1.313 (2)
C2—N2	1.291 (2)	C9—N3	1.376 (2)
C2—C3	1.454 (2)	C9—S1	1.6792 (18)
C3—C4	1.386 (3)	C10—N4	1.455 (2)
C3—C8	1.401 (3)	C10—H10A	0.9800
C4—C5	1.384 (3)	C10—H10B	0.9800
C4—H4	0.9500	C10—H10C	0.9800
C5—C6	1.388 (3)	N1—H1N	0.79 (3)
C5—Cl1	1.7475 (19)	N2—N3	1.345 (2)
C6—C7	1.393 (3)	N3—H3N	0.83 (3)
C6—H6	0.9500	N4—H4N	0.87 (3)
C7—C8	1.381 (3)		
O1—C1—N1	127.53 (18)	C7—C8—N1	128.59 (18)
O1—C1—C2	126.21 (17)	C3—C8—N1	109.59 (16)
N1—C1—C2	106.26 (16)	N4—C9—N3	116.50 (16)
N2—C2—C3	125.68 (16)	N4—C9—S1	126.19 (14)
N2—C2—C1	127.93 (16)	N3—C9—S1	117.30 (13)
C3—C2—C1	106.39 (15)	N4—C10—H10A	109.5
C4—C3—C8	120.74 (17)	N4—C10—H10B	109.5
C4—C3—C2	132.84 (17)	H10A—C10—H10B	109.5
C8—C3—C2	106.41 (16)	N4—C10—H10C	109.5
C5—C4—C3	117.17 (17)	H10A—C10—H10C	109.5
C5—C4—H4	121.4	H10B—C10—H10C	109.5
C3—C4—H4	121.4	C1—N1—C8	111.32 (16)
C4—C5—C6	122.28 (18)	C1—N1—H1N	123.1 (19)
C4—C5—Cl1	118.75 (15)	C8—N1—H1N	125.5 (19)
C6—C5—Cl1	118.95 (15)	C2—N2—N3	117.21 (15)
C5—C6—C7	120.64 (18)	N2—N3—C9	120.21 (15)
C5—C6—H6	119.7	N2—N3—H3N	121.4 (17)

C7—C6—H6	119.7	C9—N3—H3N	118.2 (17)
C8—C7—C6	117.32 (17)	C9—N4—C10	123.53 (17)
C8—C7—H7	121.3	C9—N4—H4N	118.4 (17)
C6—C7—H7	121.3	C10—N4—H4N	117.8 (17)
C7—C8—C3	121.81 (18)		

O1—C1—C2—N2	−2.4 (3)	C6—C7—C8—N1	−179.15 (17)
N1—C1—C2—N2	178.37 (18)	C4—C3—C8—C7	−2.1 (3)
O1—C1—C2—C3	178.15 (18)	C2—C3—C8—C7	178.33 (16)
N1—C1—C2—C3	−1.04 (19)	C4—C3—C8—N1	177.97 (16)
N2—C2—C3—C4	2.7 (3)	C2—C3—C8—N1	−1.55 (19)
C1—C2—C3—C4	−177.88 (19)	O1—C1—N1—C8	−179.07 (18)
N2—C2—C3—C8	−177.86 (17)	C2—C1—N1—C8	0.1 (2)
C1—C2—C3—C8	1.57 (19)	C7—C8—N1—C1	−178.94 (18)
C8—C3—C4—C5	1.1 (2)	C3—C8—N1—C1	0.9 (2)
C2—C3—C4—C5	−179.57 (18)	C3—C2—N2—N3	178.33 (16)
C3—C4—C5—C6	1.1 (3)	C1—C2—N2—N3	−1.0 (3)
C3—C4—C5—Cl1	−177.22 (13)	C2—N2—N3—C9	177.74 (16)
C4—C5—C6—C7	−2.3 (3)	N4—C9—N3—N2	−0.8 (2)
Cl1—C5—C6—C7	176.06 (14)	S1—C9—N3—N2	179.76 (13)
C5—C6—C7—C8	1.2 (3)	N3—C9—N4—C10	178.17 (17)
C6—C7—C8—C3	1.0 (3)	S1—C9—N4—C10	−2.4 (3)

Hydrogen-bond geometry (Å, º)

Cg is the centroid of the C3–C8 ring.

D—H···*A*	*D*—H	H···*A*	*D*···*A*	*D*—H···*A*
N3—H3*N*···O1	0.83 (2)	2.12 (3)	2.756 (2)	134 (2)
N1—H1*N*···O1^{i}	0.79 (2)	2.04 (3)	2.824 (2)	175 (2)
N4—H4*N*···S1^{ii}	0.88 (3)	2.72 (3)	3.518 (2)	152 (2)
C6—H6···*Cg*^{iii}	0.95	2.61	3.410 (2)	142

Symmetry codes: (i) *x*+1/2, −*y*+3/2, −*z*+1; (ii) −*x*, *y*−1/2, −*z*+3/2; (iii) *x*+1/2, −*y*+1/2, −*z*+1.